iScience

Article

Succinate supplementation alleviates liver cancer by inhibiting the FN1/SQLE axis-mediated cholesterol biosynthesis

Graphical abstract

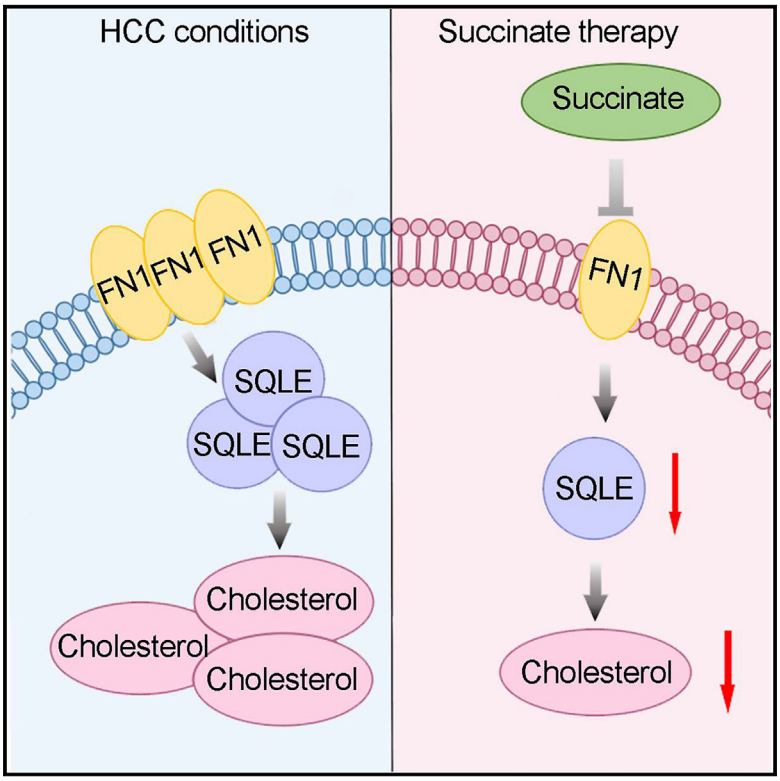

Highlights

- The concentration of succinate is decreased in HCC tissues
- Succinate supplementation demonstrates therapeutic effects on liver cancer
- Fibronectin 1 (FN1) protein mediated the anti-proliferation function of exogenous succinate
- Succinate inhibits SQLE-activated cholesterol biosynthesis by reducing FN1 expression

Authors

Shuyuan Chang, Ayaka Tomii, Yunfei Zhou, ..., Lei Yu, Wei Sun, Dabin Liu

Correspondence

menghongxue15@163.com (H.M.), yl@hrbmu.edu.cn (L.Y.), sunwei1223@hotmail.com (W.S.), liudb526@hrbmu.edu.cn (D.L.)

In brief

Biological sciences; Cell biology; Cancer

Chang et al., 2025, iScience *28*, 111731
February 21, 2025
https://doi.org/10.1016/j.isci.2024.111731

CellPress

iScience

CellPress
OPEN ACCESS

Article

Succinate supplementation alleviates liver cancer by inhibiting the FN1/SQLE axis-mediated cholesterol biosynthesis

Shuyuan Chang,[1,5] Ayaka Tomii,[2,5] Yunfei Zhou,[1,5] Xun Yang,[1] Yihong Dong,[1] Jun Yan,[1] Aodi Wu,[1] Yumeng Wang,[1] Qingxin Zhang,[1] Hongxue Meng,[3,*] Lei Yu,[2,*] Wei Sun,[4,*] and Dabin Liu[1,6,*]

[1]NHC Key Laboratory of Molecular Probes and Targeted Diagnosis and Therapy, The Fourth Hospital of Harbin Medical University, Harbin 15001, China

[2]Department of Infectious Disease, The Fourth Hospital of Harbin Medical University, Harbin 150001, China

[3]Department of Pathology, Harbin Medical University Cancer Hospital, Harbin, China

[4]Peking University People's Hospital, Peking University Institute of Hematology, National Clinical Research Center for Hematologic Disease, Beijing Key Laboratory of Hematopoietic Stem Cell Transplantation, Beijing, China

[5]These authors contributed equally

[6]Lead contact

*Correspondence: menghongxue15@163.com (H.M.), yl@hrbmu.edu.cn (L.Y.), sunwei1223@hotmail.com (W.S.), liudb526@hrbmu.edu.cn (D.L.)

https://doi.org/10.1016/j.isci.2024.111731

SUMMARY

Succinate is a crucial metabolite in the TCA cycle and contributes to cancer development. However, the role of exogenous succinate in hepatocellular carcinoma (HCC) is unclear. Here, we report that the concentration of succinate in HCC tissues is lower compared to adjacent normal tissues, as determined by spatial metabolomics and quantitative metabolomics analysis. Succinate supplementation exhibits an anti-tumorigenic effect, inhibiting cell proliferation and colony formation in liver cancer cells but not in non-tumor LO2 cells. Additionally, succinate supplementation significantly reduces tumor formation in xenograft nude mice models and carcinogen-induced WT mice models. The anti-tumorigenic function of succinate is mechanistically mediated by FN1-activated SQLE-related cholesterol biosynthesis. Our study demonstrates that exogenous succinate acts as a cholesterol biosynthesis inhibitor to suppress HCC both *in vitro* and *in vivo*, highlighting its potential therapeutic applications.

INTRODUCTION

Liver cancer is a leading cause of cancer-related death worldwide, accounting for 866,136 new cases and 758,726 deaths globally in 2022.[1] In China, approximately 367,700 new liver cancer cases and 316,500 deaths were reported in 2022.[2] Metabolic disorders are critical for the development of hepatocellular carcinoma (HCC).[3] Certain well-known genes related to tumors, such as p53,[4,5] PTEN,[6] and Myc,[7] can induce liver metabolism reprogramming and influence HCC progression. Metabolism-related genes, including pyruvate kinase M2 (PKM2), which is a vital regulator of the Warburg effect, can impair glucose metabolism and promote HCC growth.[8] Squalene epoxidase (SQLE), a cholesterol biosynthesis regulator, contributes to the development of non-alcoholic fatty liver disease-associated liver cancer (NAFLD-HCC) by activating the PI3K/AKT/mTOR pathway.[9–11] Additionally, certain metabolites involved in PUFA, one-carbon metabolism, and amino acid metabolism can also impact HCC development.[12–14] However, further investigation is needed to determine the precise role of specific metabolites in HCC. Succinate is a crucial metabolite in the tricarboxylic acid cycle and acts as a substrate for succinate dehydrogenase.[15] Succinate has shown a wide range of metabolic benefits, including increasing thermogenesis in fat cells and reducing macrophage inflammation caused by obesity.[16–18] However, the specific role of succinate in tumorigenesis is still not fully understood. Some research suggests that mutations in succinate dehydrogenase may result in the accumulation of succinate in tumors, leading to metabolic changes and supporting tumor growth.[19] Nevertheless, based on spatial metabolomics and quantitative metabolomics analysis of liver cancer tissues, we observed a significant decrease in the concentration of succinate within liver cancer. This suggests that succinate may have organ-specific effects during cancer development. In this study, we investigate the role of succinate supplementation in inhibiting liver cancer cell proliferation *in vitro*. We also observed reduced tumor development in xenograft models and in DEN-injected WT mice models. Mechanism studies suggest that succinate addition inhibits the FN1/SQLE signal, resulting in a reduced intracellular cholesterol concentration and suppression of HCC development.

RESULTS

The concentration of succinate is lower in HCC

We collected seven pairs of liver cancer tissue samples and performed spatial proteomic sequencing (Figure 1A). KEGG

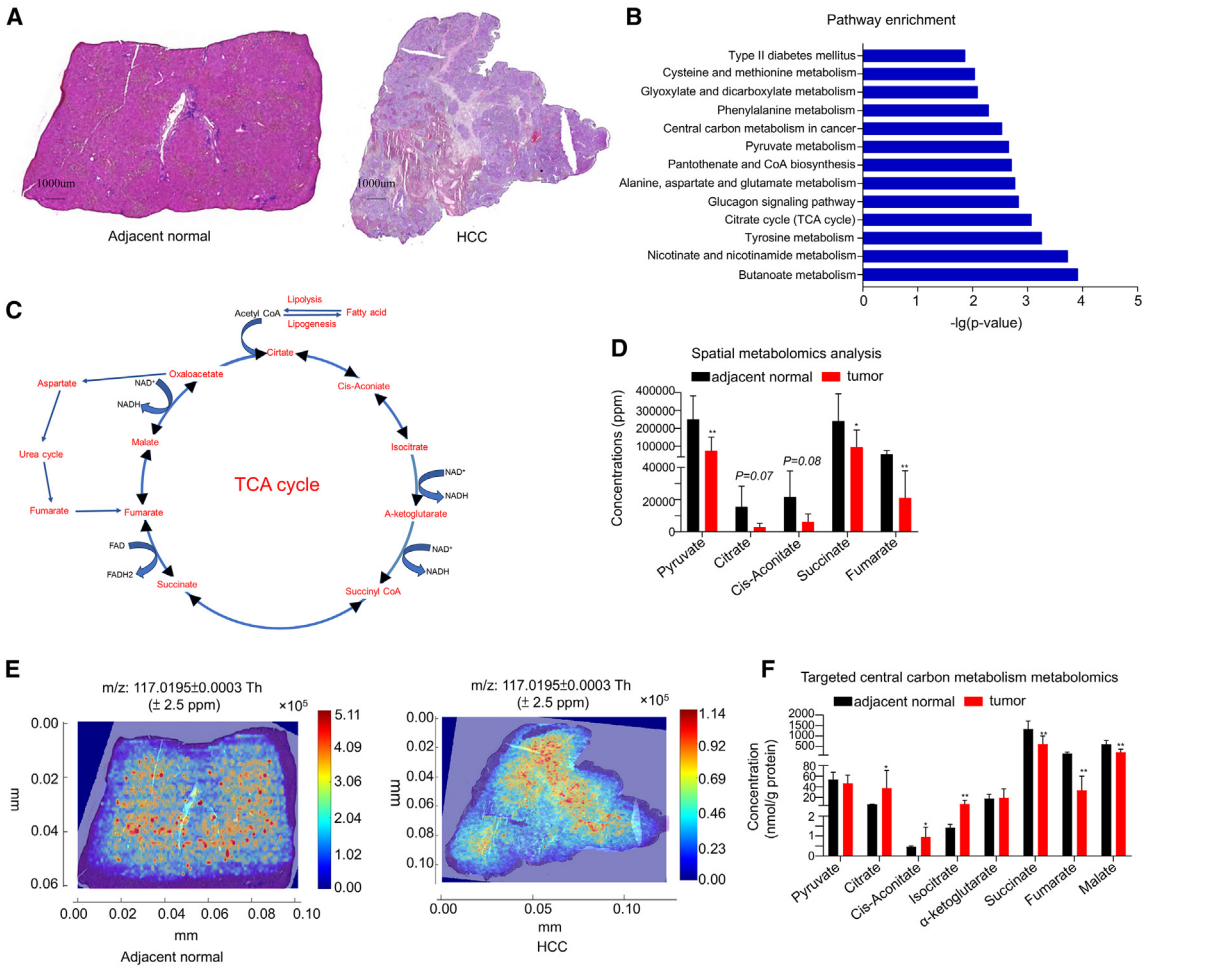

Figure 1. The concentration of succinate is lower in HCC

HCC tissues, along with paired adjacent normal tissues, were collected for spatial metabolomics analysis (A–E). All samples were initially confirmed using H&E staining.

(A) Representative image of H&E staining of these samples.

(B) KEGG pathway analysis of the results of spatial metabolomics sequencing.

(C) Images of schematic representation of the metabolites in the TCA cycle.

(D) The concentration of the TCA cycle metabolites in HCC.

(E) Representative image of succinate concentration in HCC tissues compared to adjacent normal tissue.

(F) The concentration of the TCA cycle metabolites in HCC was validated by the targeted central carbon metabolism metabolomics. Data are represented as means ± SEM.

*$p < 0.05$, **$p < 0.01$.

pathway analysis demonstrated significant changes in nicotinate and nicotinamide metabolism, TCA cycle, and several amino acid metabolism pathways in HCC compared to adjacent tissues (Figure 1B). Specifically, several metabolites of the TCA cycle (Figure 1C), such as the levels of pyruvate, succinate, and fumarate, were significantly decreased in HCC tissue, while citrate and *cis*-aconitate showed a noticeable decreasing trend (Figures 1D, 1E, and S1A; Table S2). To confirm these findings, targeted central carbon metabolism metabolomics were conducted by using nine pairs of HCC and adjacent normal tissues. The results also revealed a significant decrease in the levels of succinate and fumarate in liver cancer tissues (Figures 1F and S1B; Table S3), suggesting a certain role of succinate and fumarate in the occurrence and development of liver cancer.

Succinate addition suppresses cell growth, colony formation, and migration in HCC cells

To investigate the role of specific metabolites in HCC development, we treated three liver cancer cell lines (SK-Hep1, PLC/PRF/5, and MHCC97H) and one non-cancer cell line (LO2) with succinate, fumarate, malate or PBS. Here, LO2 cells were used as a negative control to select the metabolites that have a specific role in liver cancer. The IC50 of succinate for LO2 (IC50 = 1.202 mg/mL) was significantly higher than that of MHCC97H

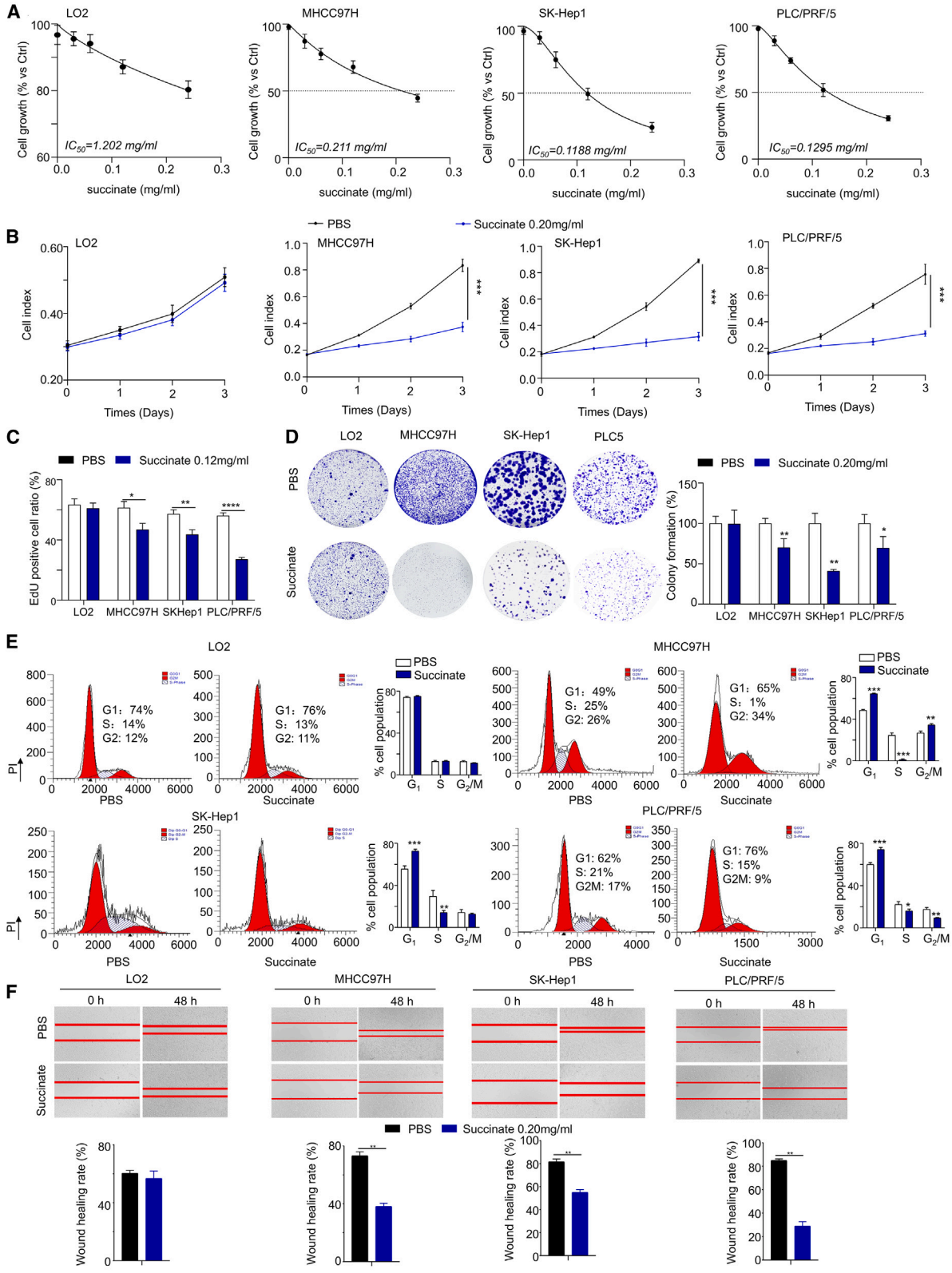

(legend on next page)

(IC50 = 0.211 mg/mL), SK-Hep1 (IC50 = 0.1188 mg/mL), and PLC/PRF/5 (IC50 = 0.1295 mg/mL), suggesting that succinate has specific anti-proliferation effects on liver cancer cells (Figure 2A). Meanwhile, fumarate and malate treatment showed similar IC50 in LO2 (for fumarate is 0.1089 mg/mL, for malate is 0.1375 mg/mL) compared to MHCC97H (for fumarate is 0.1632 mg/mL, for malate is 0.1935 mg/mL) and PLC/PRF/5 (for fumarate is 0.2818 mg/mL, for malate is 0.1462 mg/mL) cells (Figure S2). Collectively, succinate was used to perform cell viability analysis. Furthermore, succinate significantly suppressed the viability of SKHep1, PLC/PRF/5, and MHCC97H cell lines, as determined by MTT assay (Figure 2B), EdU analysis (Figure 2C) and colony formation assays (Figure 2D). In line with these findings, succinate addition into HCC cells showed a significantly decreased in S phase cell population, with a concomitant increase in cells in G1 phase (Figure 2E) while having no effect on LO2 cells. Moreover, monolayer wound healing assay results also indicated that succinate addition significantly suppressed the cell migration ability in HCC cell lines (Figure 2F). These results suggest that succinate addition has a specific effect on the suppression of HCC cell proliferation and migration.

Succinate supplementation suppresses HCC development *in vivo*

We next investigated the efficacy of succinate *in vivo*. Succinate supplementation (60 mg/kg body weight per day by gavage) significantly inhibited the growth of subcutaneous MHCC97H xenografts ($p < 0.01$) (Figure 3A), in terms of both tumor size and tumor weight ($p = 0.007$) (Figure 3B). Consistent with this, succinate also significantly suppressed the growth of subcutaneous PLC/PRF/5 xenografts ($p < 0.01$) and tumor weight ($p < 0.001$) (Figures 3C and 3D). We also validated the anti-tumor efficacy of succinate in WT mice injected with DEN and CCL4 treatment (Figure 3E). Succinate supplementation significantly reduced HCC formation confirmed by histological examination (H&E staining) (Figure 3F). Succinate also decreased tumor incidence (3/6 mice in the succinate group vs. 6/6 mice in the PBS group, $p < 0.01$), tumor number ($p < 0.01$), and tumor load ($p < 0.01$) (Figure 3G). Liver tissues from succinate treated mice showed lower Ki-67 scores compared to the liver tissues from PBS treated mice (Figure 3H), which is consistent with our *in vitro* observations. Moreover, serum ALT and AST levels were reduced after succinate treatment (Figure 3I), suggesting that succinate may cf. some benefit on liver injury. Succinate supplementation is therefore a promising choice that should be safe and effective for the prevention and treatment of HCC.

Succinate inhibits cell proliferation and migration via FN1 in HCC

RNA-seq analysis of succinate-treated SK-Hep1 and MHCC97H cells revealed a reduction in ABCA2, FN1, LAMA5, and others (Figure 4A). To investigate the downstream target gene of succinate, gene expression profiling in cells and mouse liver was conducted using qPCR. We found that the mRNA expression of FN1, but not ABCA2 or LAMA5, was significantly decreased in both succinate-treated HCC cells (SK-Hep1, PLC/PRF/5, and MHCC97H) and mice (Figures S3A and S3B). Western blot further confirmed that the protein expression of FN1 was reduced by succinate (0.20 mg/mL) in SK-Hep1, PLC/PRF/5, and MHCC97H (Figure 4A). Proteasome inhibitor (MG132) treatment failed to restore FN1 protein expression, indicating that succinate suppresses FN1 protein expression mainly by inhibiting its transcription (Figure 4B). Considering the possible absence of FN1 protein expression in LO2 cells, we hypothesized that succinate inhibits liver cancer cell proliferation by decreasing FN1 protein levels. To test this, we silenced FN1 using siRNA and then treated the cells with succinate. Compared to the siNC group, silencing FN1 significantly increased the IC50 of MHCC97H (siNC = 0.188 mg/mL vs. siFN1 = 0.404 mg/mL), PLC/PRF/5 (siNC = 0.134 mg/mL vs. siFN1 = 0.233 mg/mL), and SK-Hep1 (siNC = 0.169 mg/mL vs. siFN1 = 0.377 mg/mL) (Figure 4C). Furthermore, silencing FN1 prior to treatment notably ameliorated the impact of succinate on the viability and migration of MHCC97H, PLC/PRF/5, and SK-Hep1 cell lines, as determined by cell growth (Figure 4D), colony formation assays (Figure 4E) and wound healing assays (Figure 4F). These results suggest that FN1 plays an important role in the function of succinate in HCC development.

FN1 mediates the function of succinate-suppressed cholesterol biosynthesis and tumor formation

To confirm our findings, we analyzed the protein expression levels of FN1 in two HCC cohorts (our own cohort and the database OEP000321 in NODE (https://www.biosino.org/node)).[20] The protein levels of FN1 were significantly upregulated in primary HCC compared to their adjacent normal tissues in our own cohort ($n = 10$, $p < 0.001$) and in the the database OEP000321 ($n = 150$, $p < 0.001$) (Figure 5A). The upregulation of FN1 protein was validated in an independent cohort of 6 paired HCC samples (Figure 5B). KEGG pathway analysis revealed that the protein expression of FN1 in HCC is positively associated with steroid biosynthesis, ECM-receptor interaction, the cell cycle, the PI3K/AKT pathway, cholesterol metabolism, and others (Figure 5C). GSEA analysis further confirmed that FN1 expression is positively correlated with the steroid biosynthesis pathway in HCC ($p = 0.002$, NES = 2.265) (Figure 5D). Consistent with this finding, the protein expression of FN1 showed a positive correlation with SQLE in HCC ($p < 0.05$, R = 0.1601, Fudan cohort) (Figure 5E). Silencing FN1 in SK-Hep1, PLC/PRF/5 and MHCC97H cells reduced the mRNA expression of SQLE (Figure 5F), indicating that FN1 promotes cell proliferation through SQLE-mediated steroid biosynthesis in HCC. Moreover, succinate treatment markedly

Figure 2. Succinate addition suppresses cell growth, colony formation, and migration in HCC cells

(A) IC50 assay of exogenous succinate in SK-Hep1, PLC/PRF/5, MHCC97H, and LO2.

(B–F) The anti-tumorigenic effect of succinate in SK-Hep1, PLC/PRF/5, and MHCC97H cells was determined by MTT assay (B), EdU assay (C), colony formation assay (D), cell cycle analysis (E), and wound healing assay (F). Data are represented as means ± SEM.

$^{*}p < 0.05$, $^{**}p < 0.01$, $^{***}p < 0.001$.

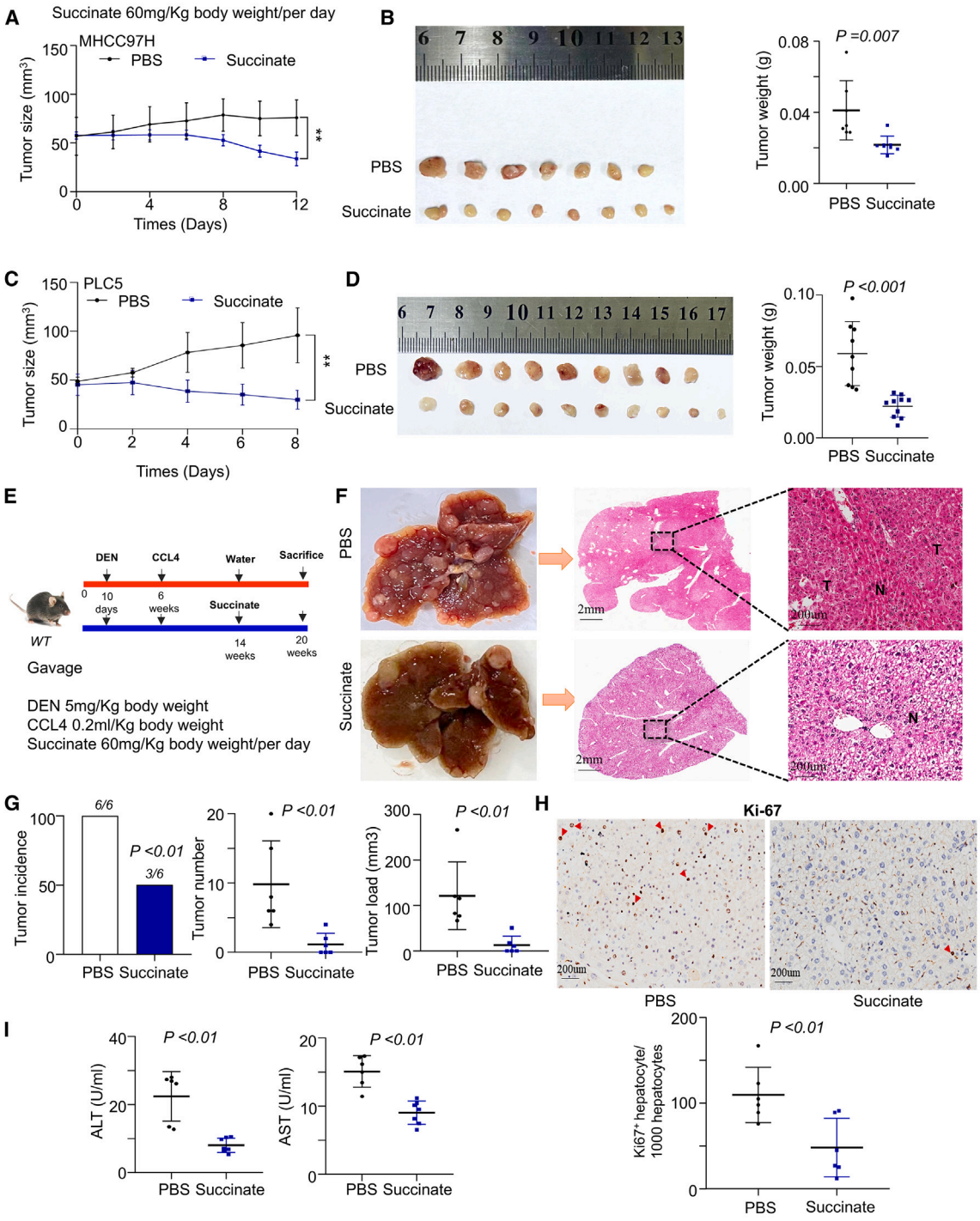

Figure 3. Succinate supplementation suppresses HCC development *in vivo*

(A and B) Succinate supplementation (60 mg/kg body weight per day by gavage) inhibited the growth of subcutaneous MHCC97H, as evidenced by a reduction in tumor volume (A) and weight (B).

(C–E) Succinate supplementation also significantly suppressed the growth of subcutaneous PLC/PRF/5 xenografts (C) and tumor weight (D). Succinate supplementation (60 mg/kg body weight per day by gavage) suppressed tumorigenesis in DEN-injected and CCL4-treated WT mice (E).

(F) H&E staining of PBS- and succinate-treated livers.

(G–I) Succinate significantly decreased tumor incidence, tumor number, and load. Ki-67 staining (H) and serum ALT and AST levels of PBS- and succinate-treated mice (I). Data are represented as means ± SEM. $^{*}p < 0.05$, $^{**}p < 0.01$.

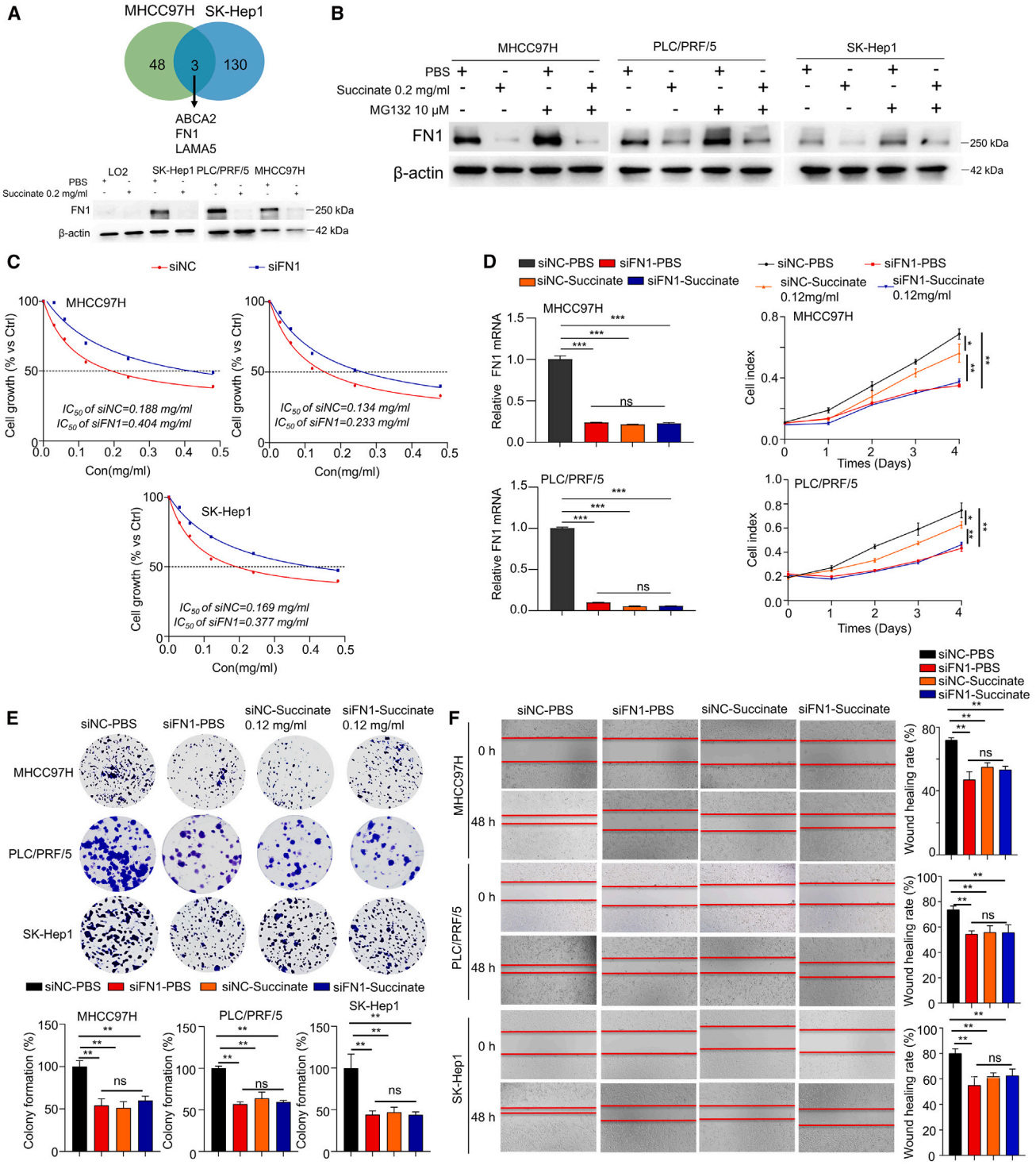

Figure 4. Succinate inhibits cell proliferation and migration via FN1 in HCC

(A) RNA-seq and western blot analysis of PBS- and succinate-treated SK-Hep1 and MHCC97H cells.

(B) Representative western blot results showed that succinate treatment cannot influence FN1 protein degradation.

(C) IC50 assay of succinate in siNC and siFN1 cells.

(D–F) (D) MTT, (E) colony formation analysis and (F) wound healing assay of the effects of succinate in FN1 silenced liver cancer cells. Data are represented as means ± SEM.

*$p < 0.05$, **$p < 0.01$, ***$p < 0.001$.

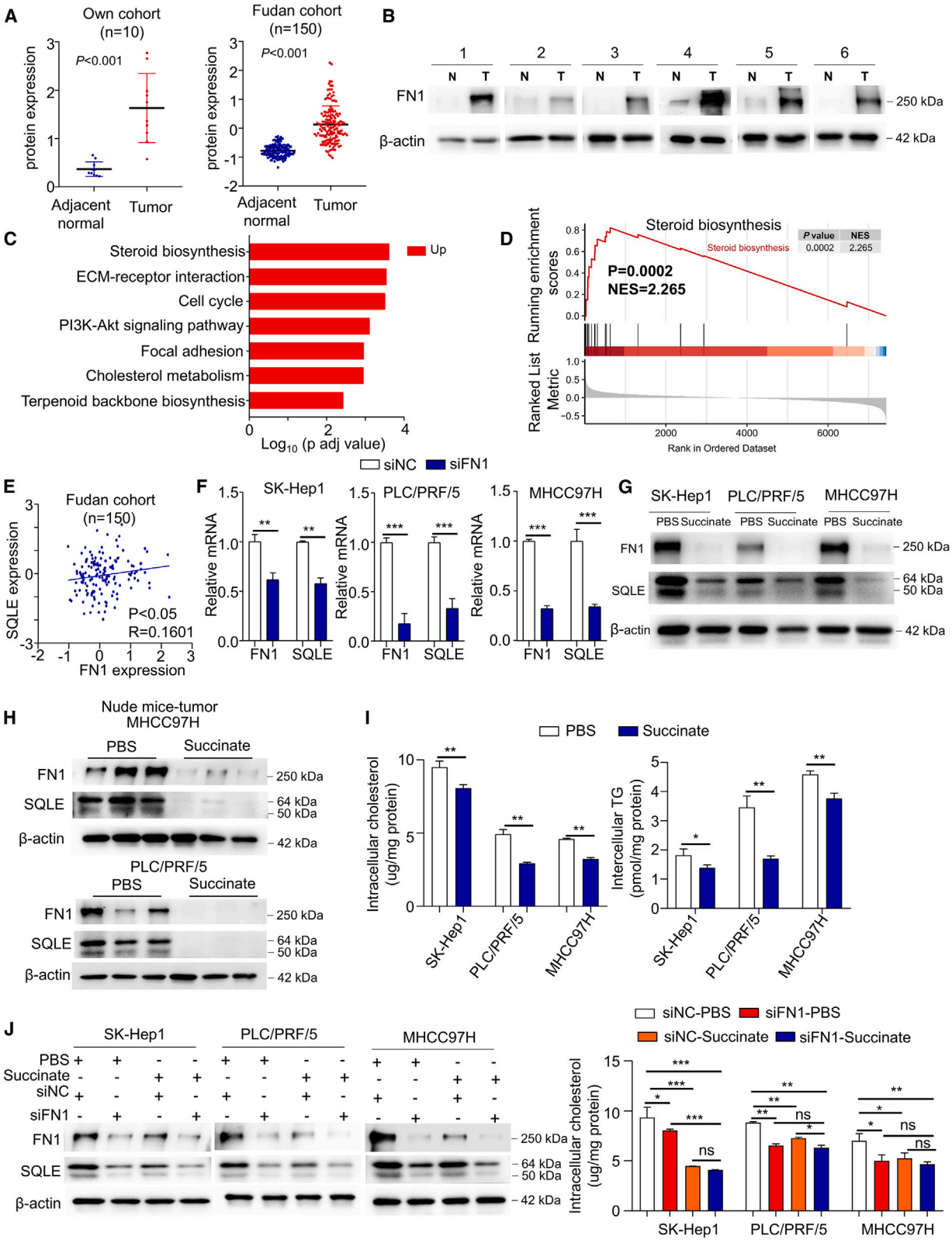

(legend on next page)

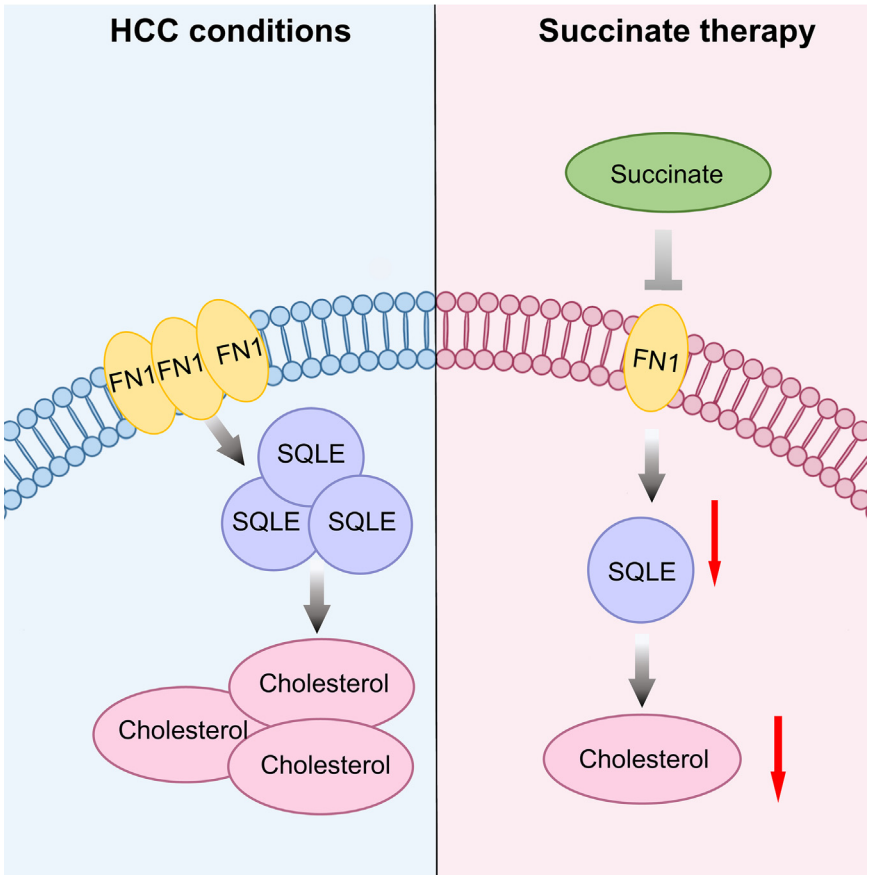

Figure 6. Schematic diagram of succinate supplementation ameliorated HCC development

FN1 promotes HCC cell growth by activating SQLE, which further activates cholesterol biosynthesis. The anti-tumorigenic effect of succinate supplementation is mediated by the FN1/SQLE axis, resulting in decreased cholesterol concentration.

inhibited the protein expression of FN1 and SQLE in three liver cancer cells (Figure 5G) and subcutaneous MHCC97H and PLC/PRF/5 xenograft tumor models (Figure 5H). Analyses of intracellular lipid profiles also showed increased levels of high-density lipoprotein cholesterol (HDL) (Figure S4A) and decreased levels of low-density lipoprotein cholesterol (LDL) (Figure S4A), cholesterol (TC) and triglyceride (TG) in three succinate treated liver cancer cells (SK-Hep1, PLC/PRF/5 and MHCC97H) (Figure 5I), while very low-density lipoprotein (VLDL) just significantly decreased in succinate treated MHCC97H cells (Figure S4A). In keeping with this, succinate supplementation markedly decreased serum and liver TG, TC, LDL, and VLDL levels (Figure S4B). However, the effect of succinate on reduced SQLE expression and cholesterol concentration may be ameliorated by silencing FN1 in MHCC97H, PLC/PRF/5, and SK-Hep1 cells (Figure 5J). Collectively, the anti-proliferation role of succinate was mediated by FN1-regulated SQLE expression and cholesterol accumulation (Figure 6).

DISCUSSION

In this study, based on spatial metabolomics and quantitative metabolomics analysis of paired tumor and adjacent liver samples, we discovered that the concentration of succinate was significantly decreased in liver cancer tissues. Succinate addition exerts its anti-proliferation effect through reducing FN1 gene expression, resulting in SQLE-related cholesterol biosynthesis inhibition to suppress carcinogenesis in HCC cell lines. Succinate supplementation conferred a therapeutic benefit in HCC, including xenograft nude mice models and carcinogen-induced WT mice model, corroborating succinate supplementation as a therapeutic strategy in the subset of HCC.

The tricarboxylic acid cycle (TCA cycle) is crucial for cellular energy metabolism, macromolecule synthesis, and redox balance.[21] Recent studies have revealed that genes and metabolites within the TCA cycle are implicated in tumor development and progression.[22] Specifically, succinate, a significant metabolite in this cycle, plays a role in both tumor initiation and progression.[23,24] In lung cancer, succinate derived from the cancer cells activates the SUCNR1 receptor and facilitates tumor metastasis through the PI3K/AKT pathway.[19] However, data from The Cancer Genome Atlas (TCGA) indicate that SUCNR1 expression is

Figure 5. FN1 mediates the function of succinate-suppressed cholesterol biosynthesis and tumor formation

(A) FN1 protein expression in two independent HCC cohorts.
(B) Increased FN1 protein expression in human HCC was validated by western blot.
(C) KEGG analysis of FN1 protein in the Fudan cohorts.
(D) GSEA analysis of FN1 protein and the sterol biosynthesis pathway in Fudan cohorts.
(E) The protein expression of FN1 showed a positive correlation with SQLE in HCC.
(F) Silence FN1 by siRNA significantly reduce mRNA expression of SQLE.
(G and H) Succinate treatment decreases FN1 and SQLE protein expression in HCC cells (G) and xenografts mice models (H).
(I) Succinate treatment significantly decreased intracellular cholesterol and triglyceride concentration.
(J) SQLE protein expression and cholesterol concentration detection in succinate-treated and FN1-silenced HCC cells. Data are represented as means ± SEM.
$^{*}p < 0.05$, $^{**}p < 0.01$, $^{***}p < 0.001$.

considerably decreased in liver cancer, suggesting a distinct role for succinate in liver cancer. Our metabolomic study discovered that succinate is downregulated in liver cancer, and supplementing succinate inhibits tumor cell growth and formation. These findings highlight tissue-specific differences in the function of succinate, underscoring the importance of precision medicine in the development of future therapeutic strategies.

RNA sequencing and western blot analysis showed that succinate addition significantly inhibits the expression of the fibronectin (FN1) gene. FN1 is a glycoprotein that plays a crucial role in the extracellular matrix.[25] Previous studies have highlighted the importance of FN1 in tumorigenesis and malignant progression in various cancers, such as colorectal cancer, breast cancer, and gastric cancer.[26–28] However, its role in liver cancer remains unclear. In this study, we found a positive correlation between FN1 expression and several cancer-related pathways, including cholesterol biosynthesis, ECM, cell cycle, and the PI3K/AKT pathway. Furthermore, silencing FN1 resulted in suppressed cell proliferation and reduced intracellular cholesterol levels in liver cancer cells. Additionally, FN1 was found to mediate the anti-proliferative and anti-cholesterol biosynthesis effects of succinate, suggesting its involvement in the development of liver cancer.

Our findings support the idea that cholesterol has oncogenic properties.[29] SQLE is important for cholesterol biosynthesis and is a new oncogene in HCC.[10] Targeting SQLE is an effective treatment strategy for HCC.[11] In line with this, we discovered that succinate supplementation significantly decreases SQLE expression and lowers intracellular cholesterol levels. Therefore, our data reveal that extracellular succinate acts as an inhibitor of SQLE-related cholesterol biosynthesis, which is crucial for the growth of HCC cells.

The impact of our findings was strengthened by observing that the concentration of succinate was lower in HCC compared to adjacent normal tissues. Succinate supplementation showed therapeutic benefits in HCC by inhibiting FN1/SQLE-related cholesterol biosynthesis. Although the impact of succinate requires additional validation through various models, our findings endorse the concept that the supplementation with native metabolites is a promising therapeutic strategy for the management of human diseases.

In conclusion, the discovery of succinate, an integral metabolite in the TCA cycle, which is decreased in liver cancer tissue and acts as an inhibitor of cholesterol biosynthesis, could suppress liver cancer cell proliferation and tumor formation. The supplementation of extracellular succinate may represent a promising therapeutic approach for the prevention of HCC.

Limitations of the study

The study's limitation lies in the role of succinate in liver cancer. Our findings indicate that exogenous succinate exhibits therapeutic effects on liver cancer, aligning with studies on the beneficial effects of dietary succinate on improvements in glucose and insulin tolerance in WT mice.[30] However, tumor-derived succinate has been shown to act as a driver of tumor growth and metastasis.[19] Additionally, protein succinylation, mediated by succinyl CoA, contributes to HCC development.[31,32] A recent study has reported that 3-succinylated cholic acid (3-sucCA), a significant product of microbial-derived succinate, ameliorates metabolic dysfunction-associated steatohepatitis (MASH) in mice.[33] Collectively, the true role and mechanism of succinate supplementation in liver disease warrant further investigation in the future.

RESOURCE AVAILABILITY

Lead contact

Further information and requests for resources and reagents should be directed to and will be fulfilled by the lead contact, Dabin Liu (liudb526@hrbmu.edu.cn).

Materials availability

This study did not generate new unique reagents.

Data and code availability

No original code was generated in this study.
Any additional information required to reanalyze the data reported in this paper is available from the lead author.

ACKNOWLEDGMENTS

This study was supported by the National Natural Science Foundation of China (82273225, 82103258); HMU Marshal Initiative Funding (HMUMIF-21002); Science Fund Program for Young Talents of the Fourth Hospital of Harbin Medical University (HYDSYRCYJ01); Nn10 program of Harbin Medical University Cancer Hospital (Nn10 2024-05).

AUTHOR CONTRIBUTIONS

Conceptualization: H.M., L.Y., W.S., and D.L.; methodology: S.C., T.A., Y.Z., and Y.D.; investigation: S.C., T.A., Y.Z., and X.Y.; visualization: S.C. and T.A.; funding acquisition: H.M., W.S., and D.L.; project administration: Y.D., J.Y., A.W., Y.W., and Q.Z.; supervision: H.M., L.Y., W.S., and D.L.; writing—original draft: S.C. and T.A.; writing—review and editing: D.L.

DECLARATION OF INTERESTS

The authors declare that they have no competing interests.

STAR★METHODS

Detailed methods are provided in the online version of this paper and include the following:

- KEY RESOURCES TABLE
- EXPERIMENTAL MODELS AND SUBJECT DETAILS
  - Human samples
  - Xenograft models
  - DEN injection-induced HCC models
  - Cell culture
- METHOD DETAILS
  - MTT assay
  - EdU (5-ethynyl-2-deoxyuridine) assay
  - Apoptosis and cell cycle analyses
  - IC50 assay
  - Colony formation assay
  - Monolayer wound healing assay
  - Western blot analysis
  - Ki-67 staining
  - Serum ALT and AST
  - Serum AFP
  - Lipid profile analysis
  - Spatial metabolomics analysis
  - Central carbon metabolite analysis

SUPPLEMENTAL INFORMATION

Supplemental information can be found online at https://doi.org/10.1016/j.isci.2024.111731.

Received: August 1, 2024
Revised: November 3, 2024
Accepted: December 30, 2024
Published: January 2, 2025

REFERENCES

1. Li, Q., Ding, C., Cao, M., Yang, F., Yan, X., He, S., Cao, M., Zhang, S., Teng, Y., Tan, N., et al. (2024). Global epidemiology of liver cancer 2022: An emphasis on geographic disparities. Chin. Med. J. *137*, 2334–2342. https://doi.org/10.1097/CM9.0000000000003264.
2. Han, B., Zheng, R., Zeng, H., Wang, S., Sun, K., Chen, R., Li, L., Wei, W., and He, J. (2024). Cancer incidence and mortality in China, 2022. J. Natl. Cancer Cent. *4*, 47–53. https://doi.org/10.1016/j.jncc.2024.01.006.
3. Tenen, D.G., Chai, L., and Tan, J.L. (2021). Metabolic alterations and vulnerabilities in hepatocellular carcinoma. Gastroenterol. Rep. *9*, 1–13. https://doi.org/10.1093/gastro/goaa066.
4. Zhu, Y., Gu, L., Lin, X., Zhou, X., Lu, B., Liu, C., Li, Y., Prochownik, E.V., Karin, M., Wang, F., and Li, Y. (2023). P53 deficiency affects cholesterol esterification to exacerbate hepatocarcinogenesis. Hepatology *77*, 1499–1511. https://doi.org/10.1002/hep.32518.
5. Moon, S.H., Huang, C.H., Houlihan, S.L., Regunath, K., Freed-Pastor, W.A., Morris, J.P., 4th, Tschaharganeh, D.F., Kastenhuber, E.R., Barsotti, A.M., Culp-Hill, R., et al. (2019). p53 Represses the Mevalonate Pathway to Mediate Tumor Suppression. Cell *176*, 564–580.e19. https://doi.org/10.1016/j.cell.2018.11.011.
6. Ortega-Molina, A., and Serrano, M. (2013). PTEN in cancer, metabolism, and aging. Trends Endocrinol. Metabol. *24*, 184–189. https://doi.org/10.1016/j.tem.2012.11.002.
7. Stine, Z.E., Walton, Z.E., Altman, B.J., Hsieh, A.L., and Dang, C.V. (2015). MYC, Metabolism, and Cancer. Cancer Discov. *5*, 1024–1039. https://doi.org/10.1158/2159-8290.CD-15-0507.
8. Hou, P.P., Luo, L.J., Chen, H.Z., Chen, Q.T., Bian, X.L., Wu, S.F., Zhou, J.X., Zhao, W.X., Liu, J.M., Wang, X.M., et al. (2020). Ectosomal PKM2 Promotes HCC by Inducing Macrophage Differentiation and Remodeling the Tumor Microenvironment. Mol. Cell *78*, 1192–1206.e10. https://doi.org/10.1016/j.molcel.2020.05.004.
9. Liu, D., Wong, C.C., Zhou, Y., Li, C., Chen, H., Ji, F., Go, M.Y.Y., Wang, F., Su, H., Wei, H., et al. (2021). Squalene Epoxidase Induces Nonalcoholic Steatohepatitis Via Binding to Carbonic Anhydrase III and is a Therapeutic Target. Gastroenterology *160*, 2467–2482.e3. https://doi.org/10.1053/j.gastro.2021.02.051.
10. Liu, D., Wong, C.C., Fu, L., Chen, H., Zhao, L., Li, C., Zhou, Y., Zhang, Y., Xu, W., Yang, Y., et al. (2018). Squalene epoxidase drives NAFLD-induced hepatocellular carcinoma and is a pharmaceutical target. Sci. Transl. Med. *10*, eaap9840. https://doi.org/10.1126/scitranslmed.aap9840.
11. Wen, J., Zhang, X., Wong, C.C., Zhang, Y., Pan, Y., Zhou, Y., Cheung, A.H.K., Liu, Y., Ji, F., Kang, X., et al. (2024). Targeting squalene epoxidase restores anti-PD-1 efficacy in metabolic dysfunction-associated steatohepatitis-induced hepatocellular carcinoma. Gut *73*, 2023–2036. https://doi.org/10.1136/gutjnl-2023-331117.
12. Liu, Z., Huang, H., Xie, J., Xu, Y., and Xu, C. (2024). Circulating fatty acids and risk of hepatocellular carcinoma and chronic liver disease mortality in the UK Biobank. Nat. Commun. *15*, 3707. https://doi.org/10.1038/s41467-024-47960-8.
13. Ren, X., Rong, Z., Liu, X., Gao, J., Xu, X., Zi, Y., Mu, Y., Guan, Y., Cao, Z., Zhang, Y., et al. (2022). The Protein Kinase Activity of NME7 Activates Wnt/beta-Catenin Signaling to Promote One-Carbon Metabolism in Hepatocellular Carcinoma. Cancer Res. *82*, 60–74. https://doi.org/10.1158/0008-5472.CAN-21-1020.
14. Mossmann, D., Muller, C., Park, S., Ryback, B., Colombi, M., Ritter, N., Weissenberger, D., Dazert, E., Coto-Llerena, M., Nuciforo, S., et al. (2023). Arginine reprograms metabolism in liver cancer via RBM39. Cell *186*, 5068–5083.e5023. https://doi.org/10.1016/j.cell.2023.09.011.
15. Martinez-Reyes, I., and Chandel, N.S. (2020). Mitochondrial TCA cycle metabolites control physiology and disease. Nat. Commun. *11*, 102. https://doi.org/10.1038/s41467-019-13668-3.
16. Li, X., Huang, G., Zhang, Y., Ren, Y., Zhang, R., Zhu, W., and Yu, K. (2023). Succinate signaling attenuates high-fat diet-induced metabolic disturbance and intestinal barrier dysfunction. Pharmacol. Res. *194*, 106865. https://doi.org/10.1016/j.phrs.2023.106865.
17. Zhang, W., and Lang, R. (2023). Succinate metabolism: a promising therapeutic target for inflammation, ischemia/reperfusion injury and cancer. Front. Cell Dev. Biol. *11*, 1266973. https://doi.org/10.3389/fcell.2023.1266973.
18. Mills, E., and O'Neill, L.A.J. (2014). Succinate: a metabolic signal in inflammation. Trends Cell Biol. *24*, 313–320. https://doi.org/10.1016/j.tcb.2013.11.008.
19. Wu, J.Y., Huang, T.W., Hsieh, Y.T., Wang, Y.F., Yen, C.C., Lee, G.L., Yeh, C.C., Peng, Y.J., Kuo, Y.Y., Wen, H.T., et al. (2020). Cancer-Derived Succinate Promotes Macrophage Polarization and Cancer Metastasis via Succinate Receptor. Mol. Cell *77*, 213–227.e5. https://doi.org/10.1016/j.molcel.2019.10.023.
20. Gao, Q., Zhu, H., Dong, L., Shi, W., Chen, R., Song, Z., Huang, C., Li, J., Dong, X., Zhou, Y., et al. (2019). Integrated Proteogenomic Characterization of HBV-Related Hepatocellular Carcinoma. Cell *179*, 1240.
21. MacLean, A., Legendre, F., and Appanna, V.D. (2023). The tricarboxylic acid (TCA) cycle: a malleable metabolic network to counter cellular stress. Crit. Rev. Biochem. Mol. Biol. *58*, 81–97. https://doi.org/10.1080/10409238.2023.2201945.
22. Eniafe, J., and Jiang, S. (2021). The functional roles of TCA cycle metabolites in cancer. Oncogene *40*, 3351–3363. https://doi.org/10.1038/s41388-020-01639-8.
23. Dalla Pozza, E., Dando, I., Pacchiana, R., Liboi, E., Scupoli, M.T., Donadelli, M., and Palmieri, M. (2020). Regulation of succinate dehydrogenase and role of succinate in cancer. Semin. Cell Dev. Biol. *98*, 4–14. https://doi.org/10.1016/j.semcdb.2019.04.013.
24. Jiang, S.S., Xie, Y.L., Xiao, X.Y., Kang, Z.R., Lin, X.L., Zhang, L., Li, C.S., Qian, Y., Xu, P.P., Leng, X.X., et al. (2023). Fusobacterium nucleatum-derived succinic acid induces tumor resistance to immunotherapy in colorectal cancer. Cell Host Microbe *31*, 781–797.e9. https://doi.org/10.1016/j.chom.2023.04.010.
25. Wang, H., Zhang, J., Li, H., Yu, H., Chen, S., Liu, S., Zhang, C., and He, Y. (2022). FN1 is a prognostic biomarker and correlated with immune infiltrates in gastric cancers. Front. Oncol. *12*, 918719. https://doi.org/10.3389/fonc.2022.918719.
26. Sun, X., Li, K., Hase, M., Zha, R., Feng, Y., Li, B.Y., and Yokota, H. (2022). Suppression of breast cancer-associated bone loss with osteoblast proteomes via Hsp90ab1/moesin-mediated inhibition of TGFbeta/FN1/CD44 signaling. Theranostics *12*, 929–943. https://doi.org/10.7150/thno.66148.
27. Lu, X.Q., Zhang, J.Q., Zhang, S.X., Qiao, J., Qiu, M.T., Liu, X.R., Chen, X.X., Gao, C., and Zhang, H.H. (2021). Identification of novel hub genes associated with gastric cancer using integrated bioinformatics analysis. BMC Cancer *21*, 697. https://doi.org/10.1186/s12885-021-08358-7.
28. Wang, J., Li, R., Li, M., and Wang, C. (2021). Fibronectin and colorectal cancer: signaling pathways and clinical implications. J. Recept. Signal

Transduct. Res. *41*, 313–320. https://doi.org/10.1080/10799893.2020.1817074.

29. Xiao, M., Xu, J., Wang, W., Zhang, B., Liu, J., Li, J., Xu, H., Zhao, Y., Yu, X., and Shi, S. (2023). Functional significance of cholesterol metabolism in cancer: from threat to treatment. Exp. Mol. Med. *55*, 1982–1995. https://doi.org/10.1038/s12276-023-01079-w.
30. De Vadder, F., Kovatcheva-Datchary, P., Zitoun, C., Duchampt, A., Bäckhed, F., and Mithieux, G. (2016). Microbiota-Produced Succinate Improves Glucose Homeostasis via Intestinal Gluconeogenesis. Cell Metabol. *24*, 151–157. https://doi.org/10.1016/j.cmet.2016.06.013.
31. Bai, W., Cheng, L., Xiong, L., Wang, M., Liu, H., Yu, K., and Wang, W. (2022). Protein succinylation associated with the progress of hepatocellular carcinoma. J. Cell Mol. Med. *26*, 5702–5712. https://doi.org/10.1111/jcmm.17507.
32. Ma, W., Sun, Y., Yan, R., Zhang, P., Shen, S., Lu, H., Zhou, Z., Jiang, Z., Ye, L., Mao, Q., et al. (2024). OXCT1 functions as a succinyltransferase, contributing to hepatocellular carcinoma via succinylating LACTB. Mol. Cell *84*, 538–551.e7. https://doi.org/10.1016/j.molcel.2023.11.042.
33. Nie, Q., Luo, X., Wang, K., Ding, Y., Jia, S., Zhao, Q., Li, M., Zhang, J., Zhuo, Y., Lin, J., et al. (2024). Gut symbionts alleviate MASH through a secondary bile acid biosynthetic pathway. Cell *187*, 2717–2734.e33. https://doi.org/10.1016/j.cell.2024.03.034.
34. Liu, D., Si, B., Li, C., Mi, Z., An, X., Qin, C., Liu, W., and Tong, Y. (2011). Prokaryotic expression and purification of HA1 and HA2 polypeptides for serological analysis of the 2009 pandemic H1N1 influenza virus. J. Virol. Methods *172*, 16–21. https://doi.org/10.1016/j.jviromet.2010.12.007.
35. Liu, D., Wang, C., Li, C., Zhang, X., Zhang, B., Mi, Z., An, X., and Tong, Y. (2011). Production and characterization of a humanized single-chain antibody against human integrin alphav beta3 protein. J. Biol. Chem. *286*, 24500–24507. https://doi.org/10.1074/jbc.M110.211847.

STAR★METHODS

KEY RESOURCES TABLE

REAGENT or RESOURCE	SOURCE	IDENTIFIER
Antibodies		
Fibronectin Rabbit Polyclonal antibody	Proteintech	Cat#15613-1-AP; RRID: AB_2105691
SQLE Polyclonal antibody	Proteintech	Cat#12544-1-AP; RRID: AB_2195888
Beta Actin Monoclonal antibody	Proteintech	Cat#66009-1-Ig; RRID: AB_2687938
Biological samples		
Human HCC and adjacent normal samples (Clinical information of HCC patients see Table S1)	4th Affiliated Hospital of Harbin Medical University	N/A
Chemicals, peptides, and recombinant proteins		
Succinic acid	Aladdin	Lot#B2222467; cas:110-15-6
N-Nitrosodiethylamine	Aladdin	Lot#B2220828; cas:55-18-5
Carbon tetrachloride	Macklin	Lot#C14404678; cas:56-23-5
Fumaric acid	GLPBIO	Batch No:GC304481; cas:110-17-8
Malic acid	GLPBIO	Batch No:GC338081; cas:6915-15-7
Critical commercial assays		
Cell Cycle Staining Kit	MULTI SCIENCES	70-CCS012
BeyoClick EdU Cell proliferation Kit with TMB	Beyotime	C0088S
Triglyceride assay kit	Nanjing Jiancheng Bioengineering Institute	A110-1-1
Low-density lipoprotein cholesterol assay kit	Nanjing Jiancheng Bioengineering Institute	A113-1-1
High-density lipoprotein cholesterol assay kit	Nanjing Jiancheng Bioengineering Institute	A112-1-1
Mouse AFP ELISA Kit	Proteintech	KE10092
CH ELISA KIT	Spbio	SP12645
Glutamic-oxalacetic Transaminase (GOT/AST)Activity Assay Kit	Solarbio	BC1565
Glutamic-pyruvic Transaminase (GPT/ALT)Activity Assay Kit	Solarbio	BC1555
Human very low-density lipoprotein ELISA Kit	Spbio	SP11888
Experimental models: Cell lines		
Human:LO2 cells	ATCC	RRID: CVCL_6926
Human:SK-Hep1 cells	ATCC	HTB-52; RRID:CVCL_0525
Human: PLC/PRF/5 cells	ATCC	CRL-8024; RRID: CVCL_0485
Human: MHCC97H cells	Sun Yat-sen University	N/A; RRID: CVCL_4972
Experimental models: Organisms/strains		
Mouse:C57BL/6J	Biocytogen Pharmaceuticals (Beijing) Co., Ltd	RRID: IMSR_JAX:000664
Mouse: BALB/c nude	Beijing Vital River Laboratory Animal Technology Co., Ltd.	RRID: IMSR_CRL:194
Oligonucleotides		
siRNA targeting sequence: FN1 #1: GGCAUUAGAAGGGAUUUUUTT	This paper	N/A
Primers for SQLE, FN1, ABCA2 and LAMA5 see Table S4	This paper	N/A
Primers for Sqle, Fn1, Abca2 and Lama5 see Table S4	This paper	N/A
Software and algorithms		
Graphpad Prism 8		https://www.graphpad.com/

(*Continued on next page*)

Continued

REAGENT or RESOURCE	SOURCE	IDENTIFIER
ModFit LT 5.0		https://vsh.com/
Nikon Capture NX 2.1.1		https://www.nikon.com/
Gen5 CHS3.03		https://www.biotekinc.com/
LightCycler 480 Software		https://www.roche.com.cn/
Other		
Spatial metabolomics analysis	Shanghai Lu Ming Biotech Co., Ltd.	https://fan0liachen.qiyeku.com/index.html
Central carbon metabolite analysis	Shanghai Biotree Biotech Co., Ltd.	https://biotree.yellowurl.cn/

EXPERIMENTAL MODELS AND SUBJECT DETAILS

Human samples

HCC and adjacent normal samples used in this study were collected from patients with hepatocellular carcinoma at the 4th Affiliated Hospital of Harbin Medical University (Table S1). This study was approved by the Ethics Committee of the 4th Affiliated Hospital of Harbin Medical University, and informed consent was obtained from all patients (Approval no. 2023 - Ethical Approval No. 37).

Xenograft models

PLC/PRF/5 cells or MHCC97H cells (5×10^6 cells in 0.1 mL PBS) were injected subcutaneously into the left dorsal flank of 6-week-old male nude mice (Balb/c). Then the mice were divided into two groups: succinate (60 mg/kg/Day) and PBS in drink water. The diameter of each tumor was measured every 2 days. The mice were sacrificed at indicated days, and tumor tissues were weighed. Tumor volume (mm3) was calculated as follows: volume = (shortest diameter)^2 × (longest diameter) × 0.5. All experimental procedures were approved by the Animal Ethics Committee of the 4th Affiliated Hospital of Harbin Medical University (Approval no. 2024-DWSYLLCZ-25).

DEN injection-induced HCC models

Male wild-type mice (WT) were injected with a single dose of Diethylnitrosamine (DEN, 5 mg/kg body weight) at 10–12 days of age, and then treated with CCL4 (0.2 mL/kg body weight) twice per week by intraperitoneal injections (IP) starting at the age of 6 weeks. At the endpoint, the number of hepatic tumors was counted and confirmed by HE staining. The tumor load of the individual mouse liver was calculated with the following formula: the sum of mean diameters of all tumors in each mouse; mean diameter = (major diameter + minor diameter)/2. All experimental procedures were approved by the Animal Ethics Committee of the 4th Affiliated Hospital of Harbin Medical University (Approval no. 2024-DWSYLLCZ-25).

Cell culture

LO2, SK-Hep1 and PLC/PRF/5 cells were purchased from ATCC (Manassas, VA). MHCC97H cells were kindly provided by Professor Xiaoxing Li from Sun Yat-sen University, China. These cells were cultured in Dulbecco's modified Eagle's medium (DMEM; Gibco) supplemented with 1% Antibiotic-Antimycotic (anti-anti; Gibco) and 10% Fetal Bovine Serum (FBS; Thermo Fisher Scientific). The cells were maintained at 37°C in a humidified incubator with 5% CO2.

METHOD DETAILS

MTT assay

Cell proliferation activity was investigated using the MTT assay. Liver cells (LO2, SKHep1, PLC/PRF/5, and MHCC97H) or siFN1 transfected cells (1500/well) were plated in 96-well plates and treated with succinate (0.20 or 0.12 mg/mL in PBS) or PBS control on the second day. At the indicated time points, 20μL of the MTT (5 mg/mL) solution was added to each well and incubated for 4 h at 37°C. Then, all the medium was removed and the cells were incubated with 150 μL of DMSO for 30 min in each well. Finally, the OD570 was detected using a machine to plot the cell growth curve.

EdU (5-ethynyl-2-deoxyuridine) assay

Cell proliferation activity was also investigated using the BeyoClick EdU Cell Proliferation Kit (C0088, Beyotime) with TMB. Cells (10^4) were plated in 96-well plates and treated with succinate (0.12 mg/mL in PBS) or PBS control on the second day. Then the EdU (20 μM) was added according to the manufacturer's instructions. The results were expressed as the means ± SEM and this assay was conducted three times in triplicate.

Apoptosis and cell cycle analyses

Cell cycle and apoptosis analysis kit (C1053, Beyotime) was used to detect the cell cycle. Cells (10^6) were plated in 6-well plates and treated with succinate (0.12 mg/mL in PBS) or PBS control on the second day. After 48h treated by succinate or PBS, cells were fixed in 70% ethanol, stained with DNA staining solution (C1053, Beyotime) and propidium iodide, and analyzed by flow cytometry.

IC50 assay

Liver cells (LO2, SKHep1, PLC/PRF/5, and MHCC97H) or siFN1-transfected cells (1500/well) were plated in 96-well plates. After overnight incubation for cell adhesion, the treatment group was exposed to succinate at concentrations of 0.015 mg/mL, 0.03 mg/mL, 0.06 mg/mL, 0.12 mg/mL, 0.24 mg/mL, and 0.48 mg/mL, while the control group was treated with PBS. After 72 h of treatment, 20 μL of MTT (5 mg/mL) was added to each well and then followed the protocol of the MTT assay. The formula for calculating the inhibition rate is as follows: Inhibition Rate = (OD value of the control group - OD value of the treatment group)/OD value of the control group.

Colony formation assay

Liver cells (LO2, SKHep1, PLC/PRF/5, and MHCC97H) or siFN1 transfected cells (1500/well) were plated in 6-well plates and treated with succinate or PBS control on the second day. After culturing for 10 days, cells were fixed with 70% ethanol and stained with 1% crystal violet solution for 15 min. 6-well plates were washed with PBS and the colonies were counted. In this study, this assay was conducted three times in triplicate.

Monolayer wound healing assay

Liver cells (LO2, SKHep1, PLC/PRF/5, and MHCC97H) were plated in 6-well plates (4×10^5 cells/well). A scratch was made perpendicular to the ruler using a pipette tip on the second day and then treated with succinate or PBS control with serum-free medium. Photographs were taken at 12, 24, 36, and 48 h to assess the cells' migration ability, and the migration rate was calculated.

Western blot analysis

Western blot was performed as previously described.[34,35] Total protein samples were first separated by SDS-PAGE. Next, the protein samples were transferred onto nitrocellulose (NC) membranes (GE Healthcare). After 1 h of blocking with 3% BSA buffer at room temperature, the membrane was incubated overnight at 4°C with primary antibodies (1:1000 dilution in 1% BSA) and then incubated for 1 h at room temperature with the secondary antibody (1:10000 dilution in 1% BSA). Finally, the membranes containing the interested proteins were visualized using ECL Plus Western blotting Detection Reagents (GE Healthcare).

Ki-67 staining

Paraffin slides from succinate treated WT mice were used. Ki67 signal was assessed by anti-Ki-67 antibody (ab833; Abcam). The proliferation index was determined by counting the numbers of positive staining cells as percentages of the total number of liver cells. At least 1000 cells were counted each time.

Serum ALT and AST

The serum ALT and AST concentrations were detected by the ELISA detection kit (Solarbio). Serum from wild-type mice with PBS or succinate treatment was plated in 96-well plates (2 μL per well) and then detected according to the manufacturer's instructions.

Serum AFP

The serum AFP was detected by the mouse α-fetoprotein/AFP ELISA kit, according to the manufacturer's instructions (KE10092, Proteintech). 10 μL of serum from mice was diluted to 200 μL with Sample dilute PT1. Then the diluted samples, standard, and control were added to each microplate well for further analysis.

Lipid profile analysis

The concentrations of different metabolites were detected using the Cholesterol Quantification kit (ab65359, Abcam); or Triglyceride detection kit (ab65336, Abcam); or Low-density lipoprotein cholesterol assay kit (LDL, A113-1-1, Nanjing Jiancheng Bio); or High-density lipoprotein cholesterol assay kit (HDL, A112-1-1, Nanjing Jiancheng Bio); or Very low density lipoprotein ELISA Kit (VLDL, SP11888, spbio). Cells (10^6) or tissues (1–2 mg) or serums (2 μL) were used in this study. The results were expressed as the means ± SEM and this assay was conducted three times in triplicate.

Spatial metabolomics analysis

The embedded samples underwent spatial metabolomics analysis following the protocol developed by Shanghai Lu Ming Biotech Co., Ltd. (Shanghai, China). In summary, all embedded samples were cut into consecutive sagittal slices of approximately 10 μm using a cryostat microtome (Leica CM 1950, Leica Microsystem, Germany). These slices were then placed on a positive charge desorption plate (Thermo Scientific, U.S.A) and stored at −80°C until further analysis. Before mass spectrometry imaging (MSI) analysis, the slices were desiccated at −20°C for 1 h and then at room temperature for 2 h. Additionally, an adjacent slice was preserved

for hematoxylin-eosin (H&E) staining. Finally, the ions detected by AFADESI were annotated using the pySM 5 pipeline and the in-house SmetDB database (Lumingbio, Shanghai, China).

Central carbon metabolite analysis

The tissue samples were weighed precisely into Eppendorf tubes. Two small steel balls and 500 μL of MeOH/H2O (3/1, v/v) that had been pre-cooled at −40°C were added to the samples. The samples were vortexed for 30 s and then homogenized for 4 min at 40 Hz. They were also sonicated for 5 min in an ice-water bath. The homogenate and sonicate steps were repeated three times. After that, the samples were incubated at −40°C for 1 h and then centrifuged at 12000 rpm (RCF = 13800(×g), R = 8.6cm) and 4°C for 15 min. The supernatants (400 μL) were collected and dried by spinning. Following that, 200 μL of water was added to the dried residue as a reconstitution solution. The reconstituted samples were vortexed before being filtered through the filter membrane. They were then transferred to inserts in injection vials for HPIC-MS/MS analysis, following the protocol developed by SHANGHAI BIOTREE BIOMEDICAL TECHNOLOGY CO., LTD (Shanghai, China).

QUANTIFICATION AND STATISTICAL ANALYSIS

Statistical analysis

All statistical analyses were performed using SPSS or GraphPad software. The data were presented as means ± standard error of the mean (SEM). For multiple group comparisons, one-way analysis of variance (ANOVA) was used. For comparisons between two variables, t-tests were employed. A p-value less than 0.05 indicated statistical significance.